

Model Development for Real Time Optimal Control in Pipe Lines

Boyun Wang¹ April Warnock² Anna G. Stefanopoulou¹ and Nikolaos D. Katopodes²

Abstract—A model reference optimal control architecture for the real-time fluid control of eliminating a contaminant plume from a pipe system was introduced in an earlier paper [1]. The mathematical model for the contaminant flow, is now extended and parameterized based on computational fluid dynamic simulations of a two-dimensional (2D) channel. It is also shown, based on the computational fluid dynamics (CFD) simulations, that the 2D-based mathematical model can be used for three-dimensional (3D) pipe flow problem under certain constraints. Finally, we also derive a very simple control law of the flow rate in a boundary port that would remove a contaminant if the flow was a theoretical 2D flow. This simple control law can initialize the iterative process of computing the optimal flow based on a more complex model and real-time measurements. With the results in this article, the optimal control architecture can be tested in the real-time prototype experiments. Further improvements on the mathematical model and control algorithm can be made for real life pipe-line fluid control problems.

I. INTRODUCTION

Fluid control problems have been typically modelled by systems of partial differential equations (PDEs) and many results related to controlling a contaminant plume have been demonstrated by numerical simulations in the past. Much research was focused on the effect of boundary control actions, such as the drawing or injection of fluid via boundary ports. In 2003, Aamo *et al* in [2] demonstrated the control of mixing in a 2D channel by the boundary feedback. In 2004, L. Huang improved the optimization of the blowing and suction control on a NACA0012 airfoil in [5]. Balogh *et al* in [3] expanded the problem to 3D in 2005. A predictive control algorithm was developed in [4] eliminating a contaminant plume from a 3D channel by finite boundary ports. In order to reduce the numerical computational cost, several mathematical methods have been developed such as the Direct Numerical Simulations (DNS) in [6] and the Genetic Algorithms (GA) in [5]. This paper augments all these past efforts with a parameterizable model that can be used for on-line real-time fluid control.

The real-time predictive optimal control problem for eliminating a contaminant plume in pipe lines was formulated in our previous paper [1]. As shown in Fig. 1, the problem consists of a) observing the location of a contaminant plume by sensor arrays installed in the fully developed region, b) computing the optimal boundary control strategy through

a model reference controller and c) eliminating the contaminant plume progressively down the length of the pipe by drawing fluid at the multiple boundary ports in each control unit. Given an observed contaminant plume location Y_i s, the pre-controller quickly responds with a boundary control command Q_i s. The model reference controller iterates a fluid system math model and finds an optimal control strategy, which eliminates the contaminant while minimizing the volume of un-contaminated fluid that is drawn away through the boundary ports. The mathematical model must be solved in a short time span to ensure an optimal solution before the contaminant plume spreads out.

A computationally fast model called Ordinary Differential Equation Pathline (ODEPL) model was introduced in [1] for the simplified 2D one boundary port steady state problem. The model approximates the pathlines in the 2D channel and is referred to as Ordinary Pathline Model (OPLM) henceforth in this article. The low order model uses non-linear differential equations for computing pathlines of the contaminant as particles attracted by a magnet. Following our previous publication [1], the magnet location and strength is now calibrated systematically to emulate CFD results. Because the fluid pathlines represent spatial trajectories of the fluid particles, the approximated pathlines by the OPLM can be used to predict the trajectory of the contaminant plume.

In a computer with Intel Xeon 2.67GHz CPU and 8GB memory, the OPLM is solved using Matlab's ODE45 in less than one second while traditional CFD software (ANSYS Fluent) took one minute to find the pathlines. The OPLM

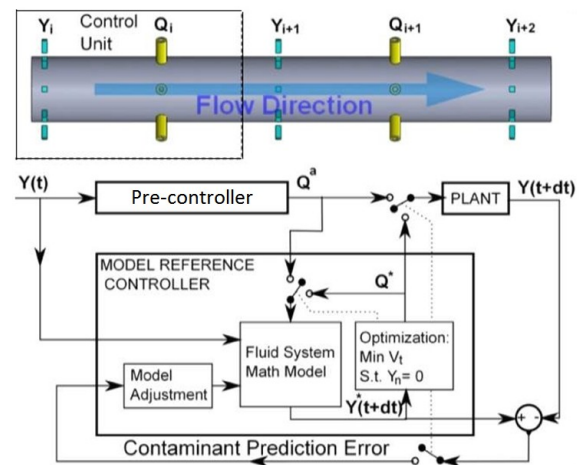


Fig. 1. Real-time optimal control architecture for eliminating a contaminant plume from a 3D pipe with multiple boundary ports and sensor arrays.

*This work was supported by NSF

¹B. Wang and A. G. Stefanopoulou are with the Department of Mechanical Engineering, University of Michigan, Ann Arbor, MI 48105, USA

²A. Warnock and N. D. Katopodes is with the Department of Civil and Environmental Engineering, University of Michigan, Ann Arbor, MI 48105, USA

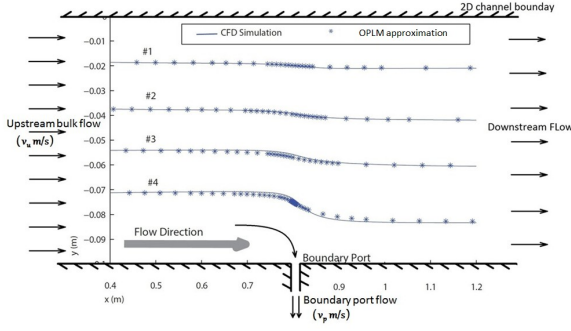


Fig. 2. OPLM approximated pathlines versus CFD Simulations in the 2D channel in [1], with an upstream flow rate of $v_u = 2$ mm/s and the boundary port drawing at $v_p = 2$ mm/s. The y-coordinate orientation is differently defined later in this article.

was compared to the CFD simulations in [1] as shown in Fig. 2 showing promising approximation results. Currently, the OPLM is only used to approximate the spatial shape of the steady state pathline but does not capture how fast the contaminant plume moves. Thus, the optimal control solution based on the OPLM only minimizes the boundary port flow rate but does not optimize the timing and duration of the control. In the future, the time-dimension will also be approximated in the OPLM in order to minimize the volume of un-contaminated fluid that is drawn by the boundary ports V_f as in Fig. 1.

In this article, as a step closer to approximating the contaminant plume velocity, the OPLM model is modified and calibrated in Section III via CFD simulations based on the 2D channel structure. To integrate the OPLM with the more realistic real-time 3D pipe prototype experiments, flow in the one port 2D channel is compared to the one port 3D pipe structure (Fig. 3) via CFD simulations in Section IV. Similarities between the two structures suggest direct application of the 2D-based OPLM for the 3D pipe problem. In Section V, a theoretical method for computing the boundary control action is formulated, which can be used as the pre-controller that will initialize the iterative process of the model reference controller shown in Fig. 1.

II. CFD SIMULATIONS SETUP

The analysis and parametrization for the OPLM model are based on CFD simulations. Laminar flow condition and incompressible fluid are assumed through out the research and are enforced in the CFD software. The 2D channel spatial discretization and fluid domain dimensions are shown in Fig. 4 based on the coordinates in Fig. 3. The grid is composed of 5580 elements with a Δx of 0.005 m, a Δy of 0.0035 m and an edge refinement at the boundary port. Steady-state simulations were carried out using water as the fluid material.

The boundary condition for the upstream edge ($x = 0$) is set as constant volume flow rate to simulate real world conditions with small changes in fluid supply. Uniform velocity profile at this boundary, v_u , is used for simplicity.

Constant volume flow rate is also used on boundary port, v_p , because volume flow rate is easier to measure and control for our prototype. The boundary condition at the downstream edge is a constant pressure.

III. OPLM REVIEW, MODIFICATION AND PARAMETRIZATION

The OPLM model has two stages and emulates the attraction on the contaminant plume by an imaginary magnet located at the boundary port. The first stage, described by (1), solves for the pathlines between the upstream boundary edge ($x = 0$) and the boundary port ($x = x_p$), where x_p is the boundary port x location. The second stage described by (2), solves for the downstream region namely after the boundary port ($x > x_p$). The differential equation states, x_1 , x_2 , x_3 and x_4 , are the x-coordinate, velocity in x-direction, y-coordinate and velocity in y-direction respectively. Given the state of a contaminant plume at the pipe section $x_1 = 0$ and a height of x_3^i with velocity $x_2 = 1$ and $x_4 = 0$, $[0, 1, x_3^i, 0]$, the pathline of the contaminant plume is approximated using the first stage at the beginning and is switched to use the second stage when x_1 reaches x_p .

Stage 1 (Upstream region, $x_1 < x_p$):

$$\begin{aligned} \dot{x}_1 &= x_2 \\ \dot{x}_2 &= \frac{G}{r\alpha} \beta(x_p - x_1) \\ \dot{x}_3 &= x_4 \left(1 - e^{c_1 \left(|x_3 - \frac{D}{2}| - \frac{D}{2} \right)} \right) \\ \dot{x}_4 &= \frac{G}{r\alpha} (y_m - x_3) \end{aligned} \quad (1)$$

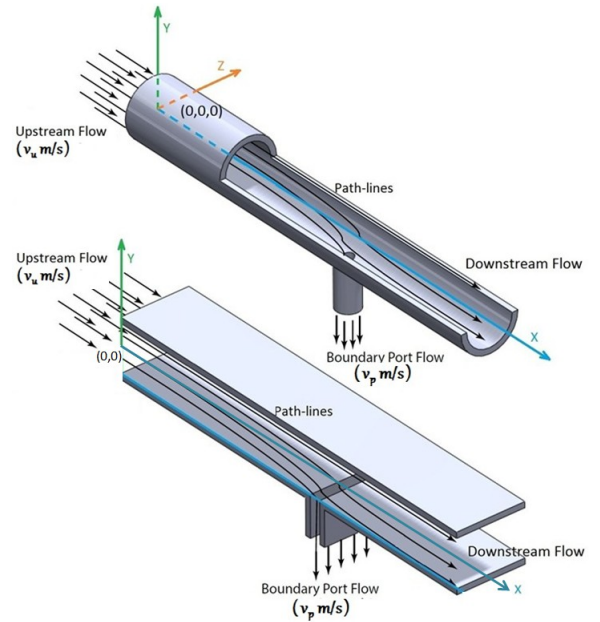


Fig. 3. One boundary port 3D pipe structure and one boundary port 2D channel structure.

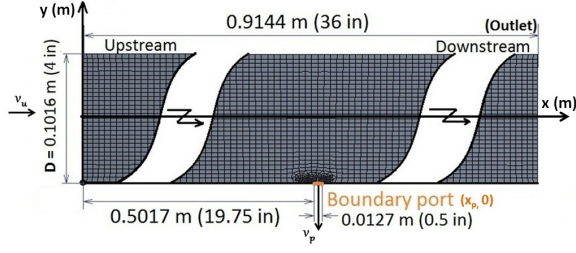


Fig. 4. One boundary port 2D channel geometry and meshing for the CFD simulations.

Stage 2 (Downstream region, $x_1 > x_p$):

$$\begin{aligned} \dot{x}_1 &= x_2 \\ \dot{x}_2 &= 0 \\ \dot{x}_3 &= x_4 \left(1 - e^{c_1 \left(|x_3 - \frac{D}{2}| - \frac{D}{2} \right)} \right) e^{-c_2(x_1 - x_p)} \\ \dot{x}_4 &= 0. \end{aligned} \quad (2)$$

As defined in (3), r represents the distance between the contaminant plume and the emulated magnet, and y_m is the virtual y-coordinate of the magnet

$$\begin{aligned} r &= \sqrt{(x_p - x_1)^2 + (y_m - x_3)^2} \\ y_m &= x_3^{ic} + \gamma \frac{D - x_3^{ic}}{x_p} x_1 \end{aligned} \quad (3)$$

where D is the channel depth.

Six tunable parameters in the OPLM, G , α , β , γ , c_1 and c_2 , are used to calibrate the approximated pathlines with the CFD ones. More information and interpretations of these parameters can be found in [1]. In the one boundary port problem, three system inputs define a pathline, upstream flow v_u , boundary port flow v_p and the observed contaminant location (y^{ic}). Despite of the promising result shown in Fig. 2, least square curve fitting for the six unknown parameters depending on the three model inputs is complex. A new variable is introduced based on CFD simulations to reduce the curve fitting complexity in this section.

A. OPLM modification

Consider the pipe section between the two sensor arrays which are installed in the fully developed flow region, one in the upstream and one downstream. The OPLM uses the observed contaminant location y^{ic} at the upstream sensor and the boundary port flow rate to predict the trajectory of the contaminant plume. Based on the CFD simulations shown in Fig. 5, where we vary v_u at the upstream boundary and v_p at the boundary port, a variable f is defined in (4) to represent the percentage of the total fluid volume drawn away through the boundary port

$$f = \frac{v_p W_p}{v_u D} \times 100\% \quad (4)$$

where $W_p = 12.7$ mm is the boundary port width.

As shown in Fig. 5, trajectories of two particles starting from two different initial positions y_1^{ic} and y_2^{ic} are taken as an

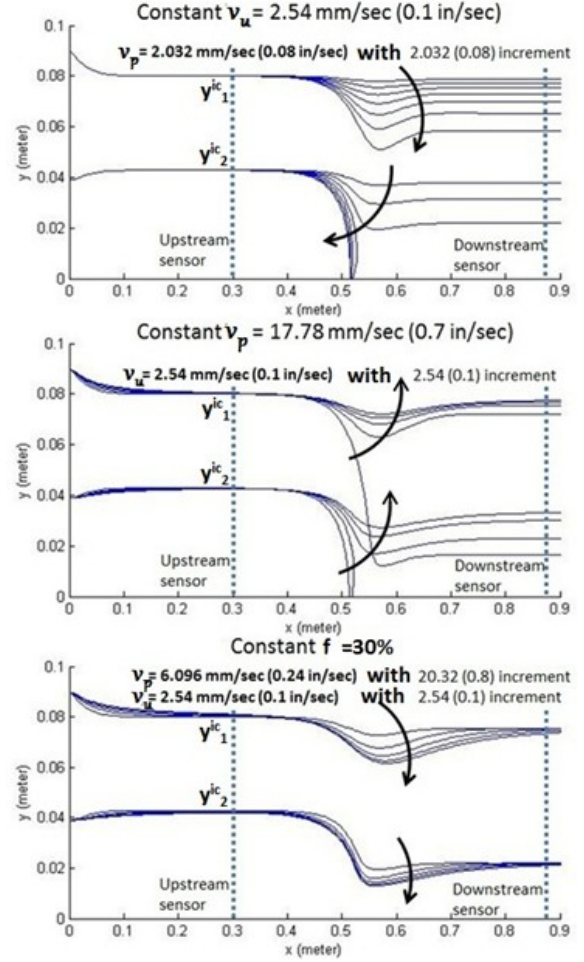


Fig. 5. Pathlines parametric study via CFD simulations, varying v_u and v_p . Dashed lines represent sensor array locations.

example. Consider the section between the two dashed lines, which represents the sensor arrays in the fully developed flow region. The pathlines tend to converge to a same position in the downstream region if the f is kept constant as shown in the third cases. So, we conclude that, under 2D laminar condition and neglecting diffusion effects, the location of a contaminant plume at the downstream fully developed region only depends on the f and y^{ic} , regardless of the pathline shape in the fluid region between the sensor arrays. This conclusion is further supported in Section V. Thus, the control algorithm only requires the f to determine if the contaminant is eliminated or not. As a result, by introducing the f , the OPLM parameters calibration is now depending on two variables, f and y^{ic} , and the associated curve fitting difficulty is reduced.

B. OPLM coefficients calibration

The OPLM parameters that depend on f and y^{ic} are calibrated based on the CFD simulations by changing the f from 10% to 90% in 10% increments and the v_u from 2.54 mm/s (0.1 in/s) to 33.02 mm/s (1.3 in/s) in 5.08 mm/s (0.2 in/s) increments.

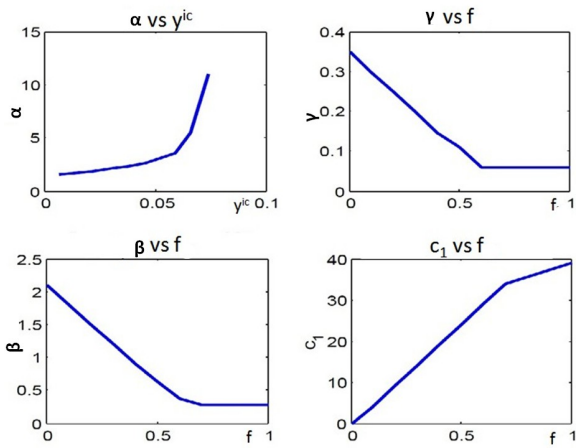


Fig. 6. OPLM coefficients calibration results. Constants $G = 5$ and $c_2 = 20$ are not shown.

Calibration analysis shows that, $G = 5$ and $c_2 = 20$ can be kept as constants, α is related with y_{ic} and β , γ , c_1 are related with f as shown in Fig. 6, which are used as lookup tables. The calibrated OPLM approximations are compared to the CFD ones in Fig. 8 which show good matching at the port upstream and downstream regions. The data in Fig. 6 may not be the optimal tuning results and the method to find the optimal parameter values is not investigated in this study.

In summary, as shown in Fig. 7, the new OPLM model first computes the f from the fluid boundary conditions the v_u and the v_p . The model parameters are then found from the lookup tables in Fig. 6. The ODE solver finally solves the two stages and gives the predicted contaminant trajectories for the control algorithm.

The resulting OPLM has two drawbacks. First, larger approximation errors occur as f increases as seen in the 60% case in Fig. 8. In the original 3D pipe problem, this can be avoided by the multiple boundary ports around the

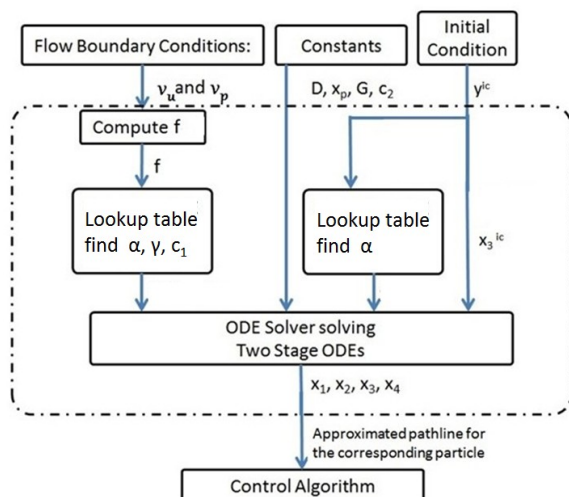


Fig. 7. Steps for approximating pathlines using the OPLM.

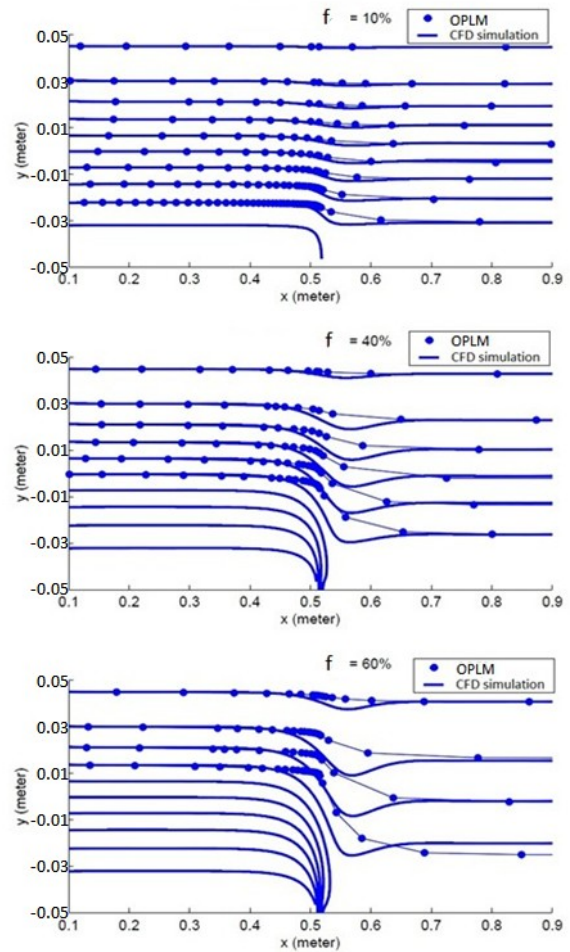


Fig. 8. OPLM approximated pathlines versus CFD simulated ones at different f value with $v_u = 2.54$ mm/s.

pipe. For example, when the contaminant plume is located at the top half of the pipe, instead of drawing fluid strongly at the bottom boundary port, ports on the top should be used. As a result, f between 0% and 50% is of greatest interest. Second, the model has a singularity at the location of the emulated magnet when the ODE solver fails. This deserves an investigation and a modification in the future.

IV. 2D CHANNEL AND 3D PIPE COMPARISON

The OPLM developed above is based on the 2D channel structure for simplicity. However, most commonly used fluid conduits in real world are pipes with circular cross-section. If the similarities between the 2D channel and the 3D pipe under laminar flow condition exist, the 2D OPLM may be directly applied for the 3D pipe control problem without increasing model dimensions. In this section, we show that the pathlines near the symmetric plane of the 3D pipe with one boundary port react very similar to the 2D channel pathlines by changing the f . The prototype experiments are planned in the future to further support the applicability of OPLM in the 3D pipe problem.

We showed in Section III-A that the pathlines converge

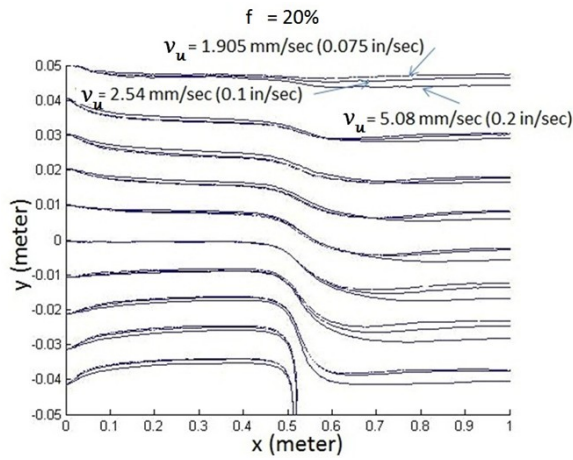


Fig. 9. Path-lines on the symmetry plane of the 3D pipe. $f = 20\%$ case. Higher deviation as bulk flow rate v_u increases.

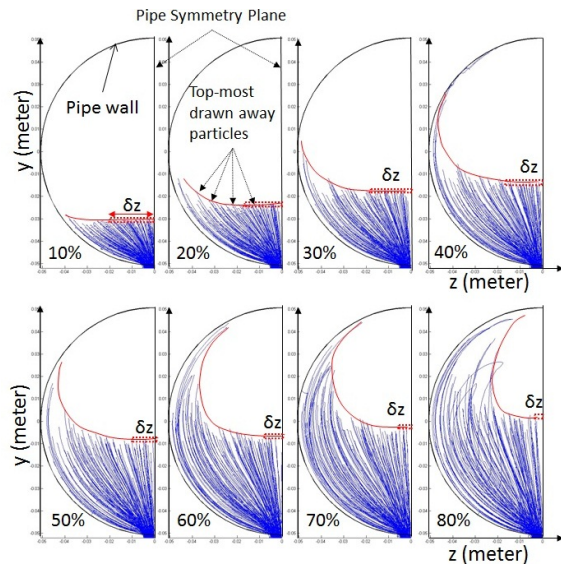


Fig. 10. Cross-section view of pathlines that is released from upstream boundary and is drawn away by the boundary port located at lowest point of the pipe. The area filled with lines represents the portion of fluid that is drawn away by the boundary port. The envelop that enclose the fluid portion can be approximated by connection top most drawn away particles indicated.

to the same y coordinates as f is kept constant. Similarly, the 3D pipe pathlines on the symmetric plane also tend to converge by keeping a constant f as shown in Fig. 9 with small error as v_u and f increase. So, the OPLM can be tuned to approximate the flow pathline on the 3D pipe symmetric plane. The model calibration for this case will be shown in our future article and the threshold of v_u and f when the approximation fails for the control algorithm will also be investigated. But, intuitively, this model error can be decreased by limiting the f control range in the control algorithm and using multiple boundary ports down the length of the pipe to gradually eliminate contaminant with smaller f at each port.

In addition, the OPLM cannot predict well the pathlines that are badly distorted near the boundary of the 3D pipe as

shown in Fig. 10. The figure shows the pathlines that start from the upstream boundary and end in the boundary port which is located at the lowest point of the cross-section. The contaminant plumes with the same y -coordinates near the symmetric plane can be drawn away, given the same control f , thus, the control algorithm can neglects the z -coordinates for a small region around the symmetric plane.

In conclusion, if a contaminant plume is observed within a small δz region, the OPLM approximates its pathline as if the contaminant is located on the symmetric plane. The same control algorithm for the 2D structure is then used to find the control solution. If the contaminant plume appears outside the δz region, the problem can be solved by the multiple boundary ports around the pipe as multiple δz s cover more area in the pipe cross-section. Further analysis of the sizing of δz by prototype experiments will be presented in our future articles.

V. FEED FORWARD CONTROL

In this section, a method for quickly providing a control solution f is formulated for the pre-controller in the control architecture shown in Fig. 1. Given an observed contaminant location y^{ic} , this formulation calculates the corresponding f regardless of how the contaminant moves. In the specific 2D laminar steady state control problem without optimizing the timing and duration of the boundary control, the solution by this formulation is in fact the optimal solution and can be used as a reference to verify the optimization algorithm.

In the fully developed 2D laminar flow channel, the velocity profile in the x direction is expressed as a parabolic function of the y -coordinate, $v_x(y)$

$$v_x(y) = -\frac{3}{4}Q\left(\frac{y^2}{h^3} - \frac{1}{h}\right) \quad (5)$$

where Q is the volume flow rate which is of unit m^2/s and $Q = v_u D$ in the upstream region for the 2D problem. The $h = \frac{D}{2}$ is the half channel depth.

Given a contaminant plume at a height of y^{ic} , the volume of fluid δV that flows beneath the contaminant pathline during time span δt can be calculated by integrating the velocity profile and is represented by the shaded area in Fig. 11. The fluid flowing above the contaminant can be found in the same way by integrating from y^{ic} to h instead

$$\begin{aligned} \delta V &= \int_{-h}^{y^{ic}} v_x(y) dy \delta t \\ &= \int_{-h}^{y^{ic}} -\frac{3}{4}Q\left(\frac{y^2}{h^3} - \frac{1}{h}\right) dy \delta t \\ &= Q\left(-\frac{y^{ic3}}{4h^3} + \frac{3y^{ic}}{4h} + \frac{1}{2}\right)\delta t. \end{aligned} \quad (6)$$

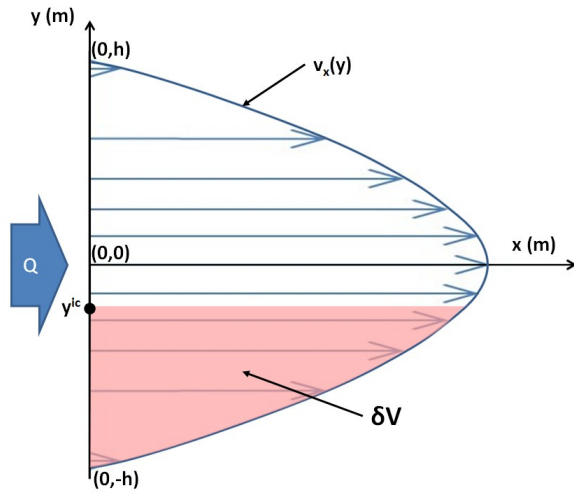


Fig. 11. Parabolic velocity profile in fully developed region. δV represents the volume of fluid that flows below the contaminant pathline that starts from y^{ic} .

The percentage of the δV out of the total upstream flow for the parabolic velocity profile is computed

$$V = \frac{\delta V}{Q\delta t} \times 100\% \quad (7)$$

$$= \left(-\frac{y^{ic3}}{4h^3} + \frac{3y^{ic}}{4h} + \frac{1}{2} \right) \times 100.\%$$

Under steady-state flow assumption, the 2D laminar flow where pathlines do not penetrate each other ensures that particles that flow above a pathline stay above it. Thus, the volume of fluid flows above the contaminant plume $Q\delta t - \delta V$ stays the same through the entire channel, regardless of the drawing by the boundary port on the channel bottom. Thus, downstream the developed region, the new contaminant location y^f can be computed with the corresponding velocity profile

$$\int_{y^{ic}}^h v_x^{upstream}(y) dy \delta t = \int_{y^f}^h v_x^{downstream}(y) dy \delta t \quad (8)$$

where the $v_x^{upstream}(y)$ is the parabolic velocity profile in upstream region. The downstream velocity profile $v_x^{downstream}(y)$ corresponds to the flow rate $Q - v_p W_p$. The v_p and W_p are boundary port flow rate and width in (4). This calculation further supports the conclusion in Section III-A. In addition, if all the fluid below the contaminant is drawn away by the boundary port, the contaminant should move to the boundary port edge.

Therefore, the control action f can be set equal to the V with the corresponding contaminant location y^{ic} from (7), and it represents that all the fluid below the contaminant is drawn away. This f value is obviously the optimal solution in the 2D one boundary port control problem, where the controller minimize the f .

VI. CONCLUSION AND FUTURE WORK

In this paper, we present and parameterize a non-linear model for predicting the pathlines of a contaminant plume in a steady-state pipe flow. The method is parameterized with a new variable f , which represents the percentage of fluid drawn away through the boundary port. The modified OPLM is calibrated and exhibits good agreement with the fluid CFD simulations for the 2D laminar flow structure. Similarities between the 2D channel flow and the 3D pipe flow encourages us to explore the applicability of the 2D based control algorithm for the more realistic 3D pipe fluid system. In addition, the control architecture previously introduced in [1] is completed with a pre-controller. With these results, a prototype experiment can be carried out to verify the control architecture and the optimal control algorithm which is based on the OPLM. Further controller modifications will be investigated based on the actual experimental data.

REFERENCES

- [1] B. Wang, A. G. Stefanopoulou and N. D. Katopodes, Model and Hardware Development for Predictive Plume Control in Pipe Lines, ASME 5th Dynamic Systems and Control Conference and 11th Motion & Vibration Conference, Fort Lauderdale, FL, 2012.
- [2] O. M. Aamo and M. Krstic, Control of Mixing by Boundary Feedback in 2D Channel Flow, Automatica, 2003, Vol. 39, Issue 9, Sep 2003, pages 1597-1606.
- [3] A. Balogh and O. M. Aamo, Optimal Mixing Enhancement in 3D Pipe Flow, IEEE Trans. Control Systems Technology, Vol. 13, No. 1, pp. 27-41, Jan 2005.
- [4] N. D. Katopodes, Control of Sudden Releases in Channel Flow, Fluid Dynamics Research, Vol. 41, Issue 6, pp. 065002, 2009.
- [5] H. Liang, Optimization of Blowing and Suction Control on NACA0012 Airfoil Using Genetic Algorithm with Diversity Control, Ph.D. dissertation, Dept. Mechanical Engineering, University of Kentucky, Lexington, KY, 2004.
- [6] T. R. Bewley, P. Moin and R. Temam, DNS-based predictive control of turbulence: an optimal benchmark for feedback algorithms, Journal of Fluid Mechanics, Vol. 447, pp. 179-225, 2001
- [7] R. Wu and N. D. Katopodes, Control of Chemical Spills by Boundary Suction, In Proc. WsEAS/IASME International Conference on Fluid Mechanics, 2006.
- [8] M. Piasecki and N. D. Katopodes, Control of Contaminant Release in Rivers. i: Adjoin Sensitivity Analysis, Journal of Hydraulic Engineering, Vol. 123, pp. 486-492, 1997.